THE CORRELATION BETWEEN GRAIN BOUNDARY CHARACTER AND INTERGRANULAR CORROSION SUSCEPTIBILITY OF 2124 ALUMINUM ALLOY

L. H. Chan[1], H. Weiland[2], S. Cheong[2], G.S. Rohrer[1], A.D. Rollett[1]

[1]Department of Materials Science and Engineering, Carnegie Mellon University, 5000 Forbes Avenue, Pittsburgh, PA 15213, USA
[2]Alcoa Technical Center, Aluminum Company of America, Alcoa Center, PA 15069, USA

ABSTRACT

The effects of grain boundary character on the intergranular corrosion susceptibility of 2124 aluminum alloy were examined. In the study, the alloy was heat treated at 540ºC and corrosion tested according to ASTM G110 standards. After obtaining grain orientations from the automated Electron Back-Scatter Diffraction (EBSD), both grain boundary character and grain boundary plane distributions were analyzed. Results show that low-angle boundaries and boundaries with a sigma-3 or sigma-7 coincident site lattice relationship tend to have a higher corrosion resistance than other random boundaries.

INTRODUCTION

Grain boundary dependent properties such as fracture and intergranular corrosion have been found to be strongly dependent on the crystallographic nature of the grain boundaries [1]. The concept of "Grain Boundary Design and Control", otherwise known as "Grain Boundary Engineering" (GBE), was first introduced by Watanabe [1]. GBE asserts that by manipulating the Grain Boundary Character Distribution (GBCD) to generate a higher fraction of low-energy Coincident Site Lattice (CSL) boundaries, the crack or corrosion resistance of the material can be improved [1]. GBE has been shown to be successful in numerous studies on nickel-based 600 alloy [2, 3], and 304 austenitic stainless steels [4-6]. In most cases, the corrosion resistance of the material increased with an increasing fraction of low CSL boundaries ($\Sigma \leq 29$), and especially with $\Sigma 3$ boundaries being the most corrosion-resistant. Other studies however, have mentioned that not all $\Sigma \leq 29$ boundaries are corrosion resistant. For example, Gertsman et al. [7] and Henrie et al. [8] have both observed that not all $\Sigma 3$ boundaries are resistant to corrosion. In this study, the effects of grain boundary character on the intergranular corrosion resistance of the 2124 aluminum alloy will be examined.

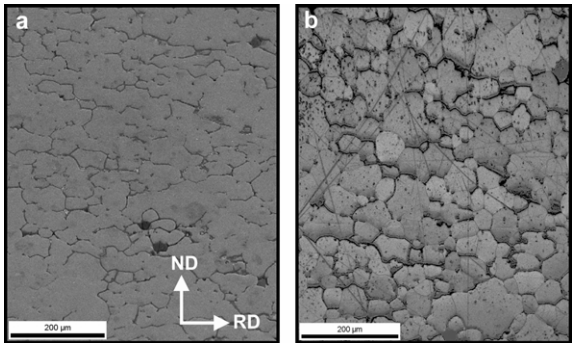

Figure 1. (a) SEM image of the corroded surface, where only the corroded boundaries are visible. (b) Image Quality map of the OIM scanned image, which shows the microstructure of the alloy.

MATERIAL PROCESSING AND CORROSION TESTING

The material used in this study was 2124 aluminum alloy; having a nominal chemical composition (wt %) of Cu: 3.8, Mg: 1.2, Mn: 0.48, Fe: 0.09, Si: 0.04, Zn: 0.04, Ti: 0.02, and balance Al. Plates of 6.3mm thickness first underwent a heat treatment at 350°C for 120 minutes followed by air cooling to remove any residual strain before it was subsequently cold rolled to 82% reduction with 23 passes through a constant speed rolling mill. After cold working, samples received a solutionizing heat treatment of 540°C for 2h followed by quenching in room temperature water immediately after removal from the box furnace. The water quenching ensures that the precipitates remain evenly distributed throughout the material. The microstructure of the alloy can be seen in the image quality map presented in Figure 1b. As can be seen in the figure, the grains are equiaxed with a non-uniform grain size distribution. All annealed samples were subjected to ASTM G110 corrosion testing, where 2.5cm x 2.5cm samples were constantly immersed in a sodium chloride and hydrogen peroxide solution for 24 h.

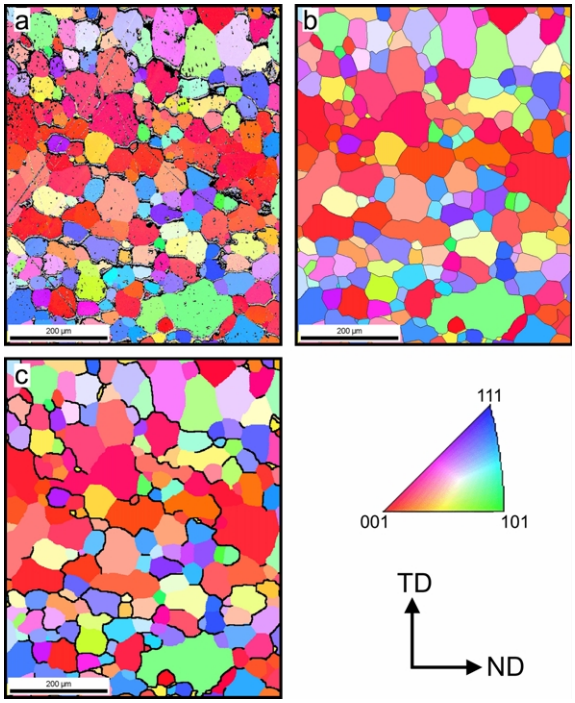

Figure 2. Inverse pole figure maps showing (a) the EBSD data as obtained from the OIM system, (b) the EBSD data that has been cleaned up with the TSL software and the grain boundary segments traced-in, and (c) the grain map with the corroded grain boundaries manually traced back onto the cleaned map.

EBSD DATA COLLECTION

The cross-sections perpendicular to the rolling plane of the corroded samples, namely the ND-RD plane, were mechanically polished for microstructural characterization through Electron Backscatter Diffraction (EBSD). All observations of grain boundary corrosion and images shown in this study were obtained on such ND-RD planes after mechanical polishing. The grain boundary microstructures were examined with a Phillips XL40 FEG instrument equipped with an EBSD indexing system provided by TexSEM Laboratories, Inc. The variables used in collecting diffraction data include: an accelerating voltage of 20kV, a working distance of approximately

17mm, and a step size of 1μm scanning on a hexagonal sampling grid. The Orientation Imaging Microscopy (OIM™) software package is used to identify CSL boundaries using Brandon's criterion [9], generate inverse pole figure maps, and extract boundary line traces that were used to determine the grain boundary plane distribution. Figure 2 shows one of the seven EBSD data sets portrayed with an inverse pole figure map, and demonstrates the method used to process the EBSD data. As a cleanup procedure in the OIM software, the scan data was grain dilated with a grain being defined as any group of pixels having more than 15 pixels with grain boundaries having a misorientation angle greater than 5°. The cleaned EBSD data was then converted into a square grid to allow the inverse pole figure map to be exported such that each pixel on the image represents one scanning step size. The corroded boundaries are traced by hand back onto the cleaned OIM image. A computer program written in C++ (see pseudo code) was then used to read in the image and categorize the boundary data into corroded and non-corroded boundary groups.

Pseudo Code: Separating corroded and non-corroded boundaries.

```
Input: exported .ang file and reconstructed boundary file from TSL software
Output: corroded boundary file and non-corroded boundary file
    scan input files for number of grain boundary segments
    read in and store confidence index (CI) values for all points from .ang file
    for each boundary segment do
        open elliptical scanning window with a=1 and c=3 pixel size
        align scanning window to have the long axis be perpendicular to and centered on
            boundary segment
        move scanning window along boundary segment in 1 pixel step size
        count up the number of black points (CI value = -1) within the elliptical window at each
            step of the moving window
        sort data and find median number of black points for the boundary segment
        if median=0
            copy boundary segment data into non-corroded boundary file
        else
            copy boundary segment data into corroded boundary file
    end for
```

RESULTS AND DISCUSSION

EBSD data results show that the area-weighted average grain size is 66.7μm, while the number-weighted average grain size is 41.8μm. Pole figures of the corroded samples show that the material has the expected recrystallization texture of face-centered cubic (FCC) materials, the cube texture, as shown in Figure 3. Volume percents of the texture components that are commonly found in FCC materials are given in Table I. The volume percents of the texture components indicate that the material generally has a random texture with the exception of having a higher volume of cube texture and lower volume of the brass texture. The probability density plot for the corroded and non-corroded boundary groups are plotted in Figure 4. The probability density of the corroded grain boundaries closely follows the McKenzie distribution for a random sample, which seems to indicate that corrosion occurs randomly on all boundaries. However, there is also a very high fraction of low-angle grain boundaries that is associated with

the non-corroded boundary group. Such results show that low angle grain boundaries clearly have a higher resistance to corrosion, which is consistent with studies performed on other aluminum alloys [10, 11].

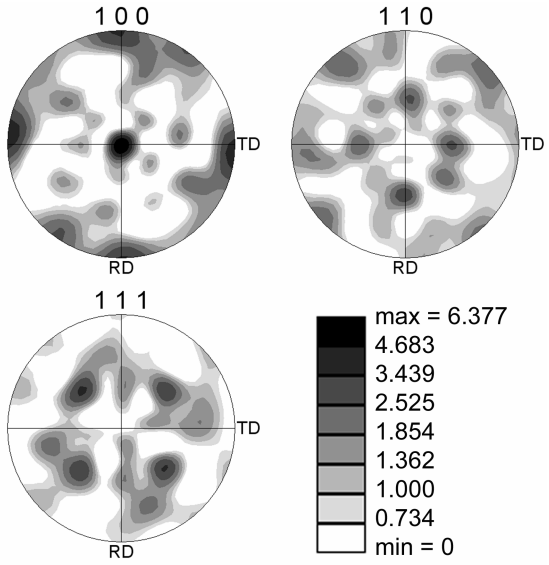

Figure 3. Example of a pole figure for one of the EBSD data sets showing cube texture.

Table I. Volume percents of typical FCC texture components as observed in the EBSD data sets compared to values expected in random texture.

Texture Components (φ1,Φ,φ2)	Experimentally Observed (Volume Percent)	Expected In Random Texture (Volume Percent)
Cube (0°, 0°, 0°)	9.44	2.45
Brass (35°, 45°, 0°)	0.61	3.23
Copper (90°, 35°, 45°)	3.90	4.29
S (50°, 35°, 70°)	7.76	7.39
Goss (0°, 45°, 0°)	1.27	2.64
Others	77.02	80.00

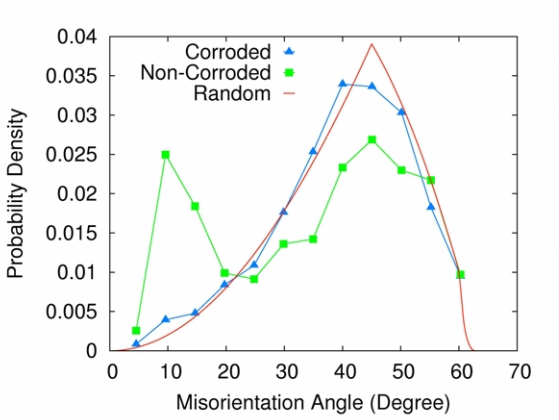

Figure 4. Probability density as a function of grain boundary misorientation angle.

Since the data collection was only limited to a 2-dimensional plane of the microstructure, the grain boundary line traces were used to produce a stereologically calculated grain boundary plane distribution in Figure 5. Exact procedures in creating the plane distributions were presented elsewhere [12, 13]. The plots for both the corroded and non-corroded boundaries appear to have a slight peak around but not at the exact (111) position. The spread of the peak near the (111) seems to indicate that the population of Σ3s found in the sample is mainly incoherent Σ3s. In comparing the two plots with each other, no obvious differences can be observed between the two distributions of planes.

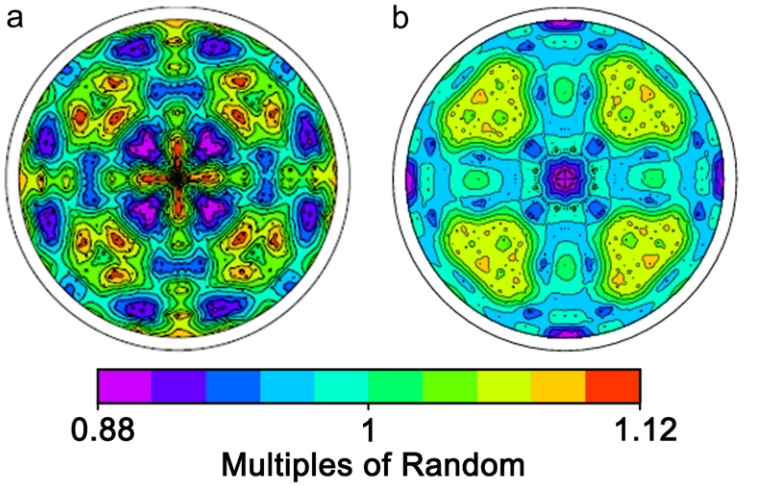

Figure 5. The distribution of grain boundary planes for the (a) corroded grain boundaries, and the (b) non-corroded grain boundaries. The data is plotted in stereographic projection along the [001].

To clarify the correlation between CSL boundaries and corrosion resistance, a more detailed analysis was conducted by identifying every $\Sigma \leq 19$ grain boundary individually in each of the EBSD data sets. The EBSD scans contained a total of 1191 grains (excluding edge grains), which corresponds to 3142 grain boundaries. In the observation, 23% of the boundaries were of $\Sigma \leq 19$ types while 49% of all the boundaries were corroded. The results from the analysis are summarized in Figure 6. The number of each type of boundary observed is included in brackets and the percentage of corrosion reported merely indicates the percent of the corresponding type of boundary that is corroded. The error bars shown in Figure 6 were produced with a hypothesis test using a binomial distribution. A binomial distribution was first created for each of the CSL boundary types, followed by taking 95% of the total area under the curve as the acceptance region. The result from the statistics test is that there is a 95% confidence that the true value lies within the limits of the error bars.

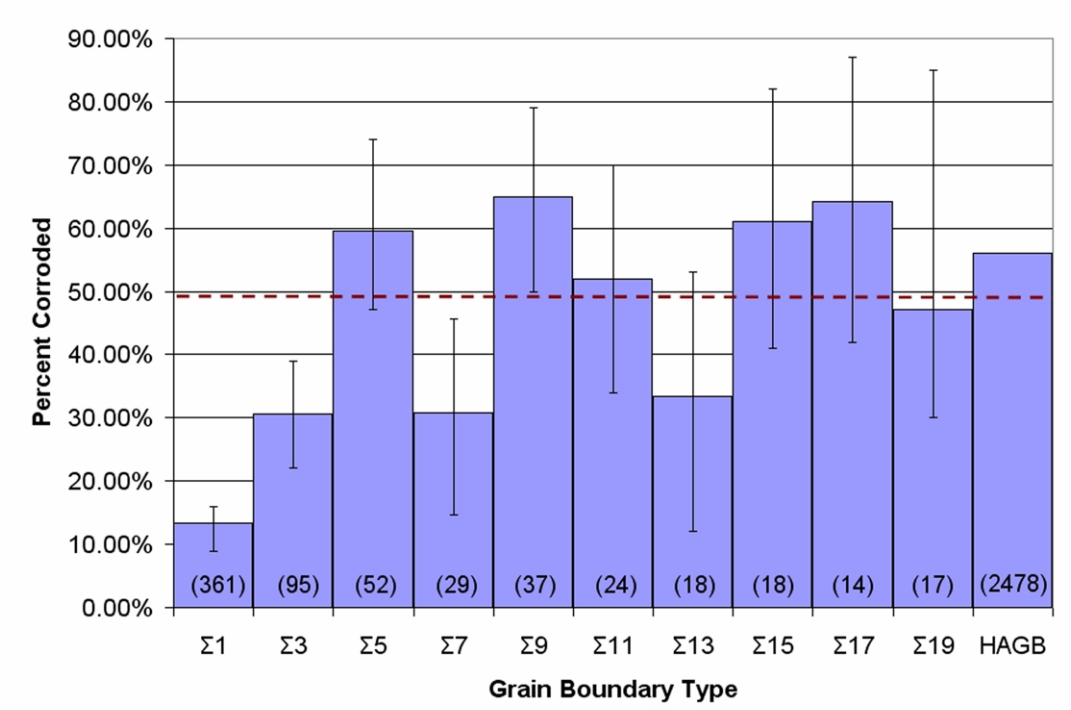

Figure 6. Results on the corrosion resistance of CSL grain boundaries. The number of grain boundaries observed for each boundary type is indicated in brackets. The dashed line across the graph shows the overall percentage of grain boundaries that were corroded. Error bars were calculated using a binomial distribution with a 95% confidence acceptance region.

From Figure 6, Σ1, 3, 7, and 13 grain boundaries appear to have a higher corrosion resistance than the other CSL boundaries analyzed. The Σ1 boundaries are usually not considered for GBE. Σ1 corresponds to a misorientation of 0° about a 111 axis, and while Brandon's criterion allows a 15° deviation from the exact CSL position, Σ1 boundaries are basically low-angle boundaries. The higher corrosion resistance of Σ13 boundaries is still uncertain since only 18 boundaries were observed and the error bars indicate that the true corrosion percentage could lie above the average corrosion line. In the interest of studying whether $\Sigma 3^n$ boundaries have higher corrosion resistance, Σ27 boundaries were also observed. However, since only six Σ27 boundaries were found in the EBSD scans, Σ27 boundaries were not included as part of the analysis.

CONCLUSION

The results from this study suggest that Σ3 and Σ7 grain boundaries tend to have a higher corrosion resistance than other low-Σ boundaries. Even though stereological methods were used to calculate the distribution of grain boundary planes, 3-dimensional serial sectioning may still be needed to fully explain why the observed Σ3 boundaries were not completely corrosion resistant. Henrie et al. suggested in their study that perhaps only coherent twin Σ3 boundaries with the lowest energy that contain 111/111 planes will truly have higher corrosion resistance [8]. Therefore, future work on studying the grain boundary planes in three dimensions will be able to clarify the true relation between Σ3 and corrosion resistance.

ACKNOWLEDGEMENTS

The EBSD work was supported by the Materials Research Science & Engineering Center (MRSEC) of the NSF at Carnegie Mellon. Alcoa Technical Center has played a vital role and provided the materials used in this research. Jason Gruber and Christopher Roberts provided computer programming assistance and helpful discussions.

REFERENCES

[1] T. Watanabe, "An Approach to Grain Boundary Design for Strong and Ductile Polycrystals" *Res Mech.*, **11**, 47-84 (1984).

[2] K.T. Aust, U. Erb,G. Palumbo, "Interface control for resistance to intergranular cracking" *Mater. Sci. Eng.*, **A176**, 329-334 (1994).

[3] P. Lin, G. Palumbo, U. Erb,K.T. Aust, "Influence of Grain Boundary Character Distribution on Sensitization and Intergranular Corrosion of Alloy 600" *Scripta Metall Mater*, **33**, 1387-1392 (1995).

[4] R. Ishibashi, T. Horiuchi, J. Kuniya, M. Yamamoto, S. Tsurekawa, H. Kokawa, T. Watanabe,T. Shoji, "Effect of Grain Boundary Character Distribution on Stress Corrosion Cracking Behavior in Austenitic Stainless Steels" *Mater Sci Forum*, **475-479**, 3863-3866 (2005).

[5] S. Tsurekawa, S. Nakamichi,T. Watanabe, "Correlation of grain boundary connectivity with grain boundary character distribution in austenitic stainless steel" *Acta Mater*, **54**, 3617-3626 (2006).

[6] H. Kokawa, M. Shimada, Z.J. Wang, Y.S. Sato,M. Michiuchi, "Grain boundary engineering for intergranular corrosion resistant austenitic stainless steel" *Key Eng Mat*, **261-263**, 1005-1010 (2004).

[7] V.Y. Gertsman,S.M. Bruemmer, "Study of Grain Boundary Character Along Intergranular Stress Corrosion Crack Paths in Austenitic Alloys" *Acta Mater*, **49**, 1589-1598 (2001).

[8] A.J. Henrie, B.L. Adams,R.J. Larsen, "Creating a model for percolation of grain boundaries in polycrystalline materials" *Mater Sci Forum*, **408-412**, 419-424 (2002).

[9] D.G. Brandon, "The Structure of High-Angle Grain Boundaries" *Acta Metall.*, **14**, 1479-1484 (1966).

[10] T. Minoda,H. Yoshida, "Effect of Grain Boundary Characterisitics on Intergranular Corrosion Resistance of 6061 Aluminum Alloy Extrusion" *Metall Mater Trans A*, **33A**, 2891-2898 (2002).

[11] B.-L. Ou, J.-G. Yang,C.-K. Yang, "Effects of Step-Quench and Aging on Mechanical Properties and Resistance to Stress Corrosion Cracking of 7050 Aluminum Alloy" *Mater T JIM*, **41**, 783-789 (2000).